Russian Journal of Biomechanics, Vol. 5, № 4: 76-89, 2001

Russian Journal of Biomechanics
www.biomech.ac.ru

PATHOMECHANICS OF MAXILLOFACIAL ASYMMETRY: COMPUTER SIMULATION OF BONE ADAPTIVE REMODELING

M. Kutsuki*, Y. Yamaguchi*, K. Yoshitake*, T. Azuma, S. Tsutsumi****

* Department of Oral and Maxillofacial Surgery, Shiga University of Medical Science, Seta Tsukinowa-cho, Otsu City, Shiga 520-2192, Japan, e-mail: kutsuki@belle.shiga-med.ac.jp
** Department of Medical Simulation Engineering, Institute for Frontier Medical Sciences, 53 Kawahara-cho Shogoin, Sakyo-ku Kyoto 606-8507, Japan

Abstract: In order to investigate the relationships among maxillofacial asymmetry, occlusal condition and bite force, remodeling simulation based on the finite element method according to Wolff's law was carried out. Four types of an abnormal occlusion model and a normal occlusion model were investigated with varying ratios of the occlusal contact area of the right and left half arches; 2.3:1, 1.4:1, 1:1, 1:1.4 and 1:2.3. The result of the remodeling simulation was compared with asymmetry of the mandible, the bite force and the occlusal contact area of patients with maxillofacial deformity. The relationships among mandibular asymmetry, bite force and occlusal contact area of the models were similar to those of the patients. It was suggested that the asymmetry of condylion-gonion and gonion-menton might occur from an imbalance of the stress distribution with malocclusion and/ or asymmetry of masticatory muscle forces.

Key words: dental biomechanics, maxillofacial asymmetry, abnormal occlusion, Woff's law, method of finite elements

Introduction

There are three types of facial deformity: congenital condition type, facial type such as a sequela from external injuries and tumors, and that due to abnormal development of the mandibular bone which can be affected by environmental factors such as abnormal tooth formation, habits, injuries and secretion [19].

Though deformity caused by the abnormal development of the mandible is the most common condition [19], there has been no detailed analysis to determine the actual causes of this condition. From a biomechanical viewpoint, the problem how much changes in the stresses exerted on the bones affect their formation has been experimentally and numerically investigated [14,17]. The masticatory muscles, which play a powerful role in clenching, cover the side of the bone, and the stresses in the bone generated by the contraction of these muscles can be considered an important factor influencing formation or deformation of the bone. The relationship between maxillofacial bone remodeling and stress has been investigated experimentally using rats, and the results demonstrate that abnormal amounts of stress exerted on the maxillofacial side of the bone cause abnormal formation and growth of the maxillofacial bone [10,12,13]. However, no study has determined the causal relationship between stress distribution and facial deformation in human.

In this paper, we simulated the imbalanced clenching stress of malocclusion and/ or of asymmetric muscles forces that might cause maxillofacial asymmetry. This was done using

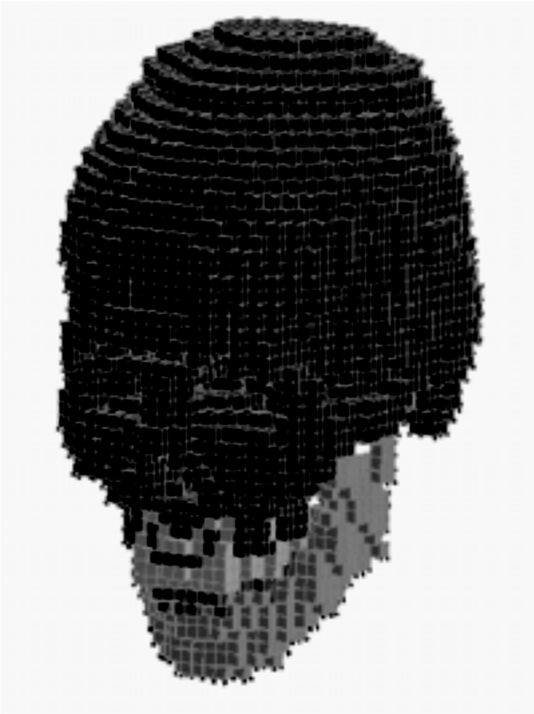

Fig. 1. A fundamental 3-D finite element model (6710 elements, 13102 nodes).

our quantitative simulation based on the finite element method, as prepared to investigate the biomechanical bone morphology adaptation process in response to stress distribution. We then compared the simulated results with a variety of bite forces and occlusal conditions from clinical cases.

Methods

(1) Preparation for a normal finite element model

A three-dimensional (3D) finite element model was prepared based on 5 mm thickness X-ray computed tomography (CT) images (SOMATOM PLUS4, Siemens) of a male adult head using a 3D construction program (The Fast Medical Meshing Program Yokogawa. Techno-Information Service inc., JAPAN). A normal standard model was constructed using bilateral symmetry. The number of nodes in the standard model was 13,102 with 6,710 elements (Fig. 1). The elements were defined as been isotropic elastic and were given material properties corresponding to each tissue (cortical bone, tooth, articular disk, condyle cartilage) which was referenced by literature data [18] (Table 1).

Table 1. Materials properties.

	Young's modulus(MPa)	Poisson's ratio
Cortical bone	13700	0,30
Tooth	30000	0,30
Articular disk	80	0,40
Cartilage	0,79	0,49

We fixed the peripheral part of the model's foramen magna as the restraints. In the spaces between the upper and lower dental arches the positions of canines, premolars and molars were connected with the materials of a low Young's modulus to reduce the effect of the tension in the simulation due to the common bonding condition of the elements. In order to investigate maxillofacial asymmetry, four types of an abnormal occlusion model along with a normal occlusion model were considered in which the ratios of the occlusal contact area of the right and left half arches varied; 2.3:1 (molars + premolars + canine: molars), 1.4:1 (molars + premolars + canine: molars + premolars), 1:1 (molars + premolars + canine: molars + premolars + canine), 1:1.4 (molars + premolars: molars + premolars + canine) and 1:2.3 (molars: molars + premolars + canine). Varying the amounts of the elements connecting the upper and lower arches made changes in the contact area.

The masticatory muscle forces according to Korioth et al. [8,9] were used, namely superficial and deep masseter, medial pterygoid, superior and inferior lateral pterygoid, anterior, middle and posterior temporalis, and anterior digastric were applied as the clenching muscle forces and as the loading conditions (Table 2).

Table 2. The muscle forces applied in the models (Modified Korioth et al., 1994).

	Symmetric muscle forces		2 times larger at left than right		2 times larger at right than left	
Muscle	Right(N)	Left	Right	Left	Right	Left
Surperficial masseter	190.4	190.4	76.2	152.3	152.3	76.2
Deep masseter	81.6	81.6	32.6	65.3	65.3	32.6
Medial pterygoid	132.8	132.8	53.1	106.2	106.2	53.1
Superior lateral ptreygoid	16.9	16.9	6.8	13.5	13.5	6.8
Anterior temporalis	154.8	154.8	61.9	123.8	123.8	61.9
Middle temporalis	92.7	92.7	37.1	74.2	74.2	37.1
Posterior temporalis	71.1	71.1	28.4	56.9	56.9	28.4
Anterior digastric	11.2	11.2	4.5	9.0	9.0	4.5
Inferior lateral pterygoid	18.1	18.1	7.2	14.4	14.4	7.2

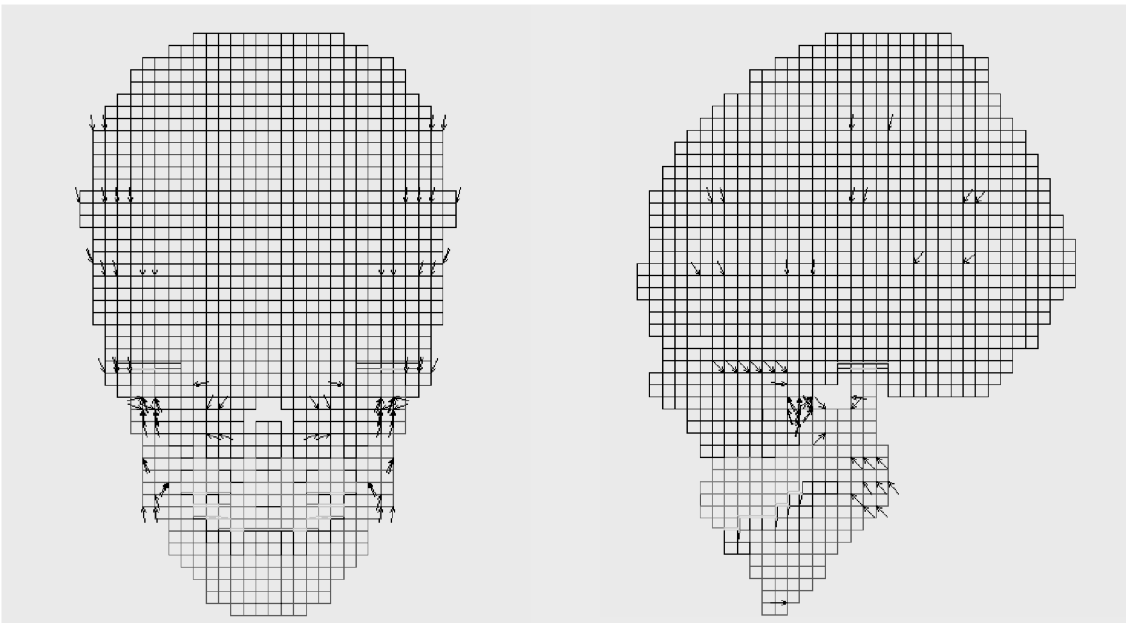

The frontal view The lateral view

Fig. 2. The loading condition.

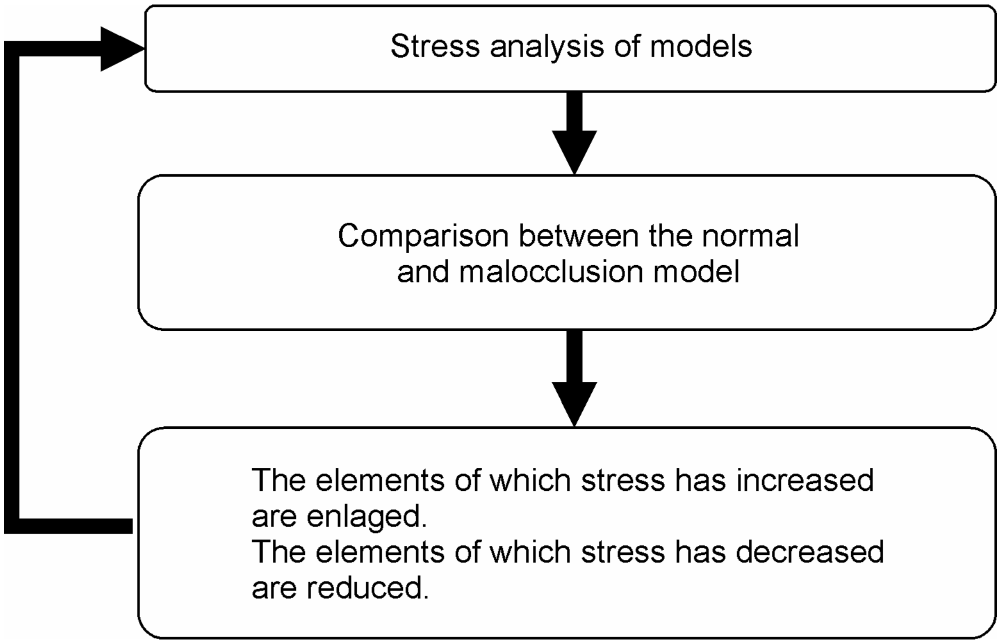

Fig. 3. The procedure of the bone remodeling simulation.

The ICP (inter cuspal position) figure employed by Korioth as the muscle strength in clenching was used here as the loading condition in our normal model. In the malocclusion model, we based the loading condition on the ICP, fixed the total force as a constant and adjusted the ratio of the right-left muscle balance in a range from 1:2 to 2:1. The direction and position of the muscle were set up according to Kamijo [5] and to the CT images (Fig. 2).

(2) Remodeling simulation

The stress distributions of the normal occlusion model with symmetric muscle forces and the abnormal occlusion models were compared using the formula in Table 3 [11]. If stress in an element was found to be higher than that of the same element in the normal condition,

Table 3. Our hypothetic relation equation between element volume change and stresses.

$$X_i = \begin{pmatrix} C_a\, Log\left(\dfrac{S_i}{2t * S_{\mathrm{hom},i}}\right) + 4C_a & \textit{when} & 2t * S_{\mathrm{hom},i} < S_i \\ C_b \left(\dfrac{S_i}{t * S_{\mathrm{hom},i}}\right)^2 & & t * S_{\mathrm{hom},i} < S_i < 2t * S_{\mathrm{hom},i} \\ 0 & & \dfrac{S_{\mathrm{hom},i}}{t} < S_i < t * S_{\mathrm{hom},i} \\ -C_b \left(\dfrac{t * S_{\mathrm{hom},i}}{S_i}\right)^2 & & \dfrac{S_{\mathrm{hom},i}}{2t} < S_i < \dfrac{S_{\mathrm{hom},i}}{t} \\ -C_a\, Log\left(\dfrac{S_{\mathrm{hom},i}}{2t * S_i}\right) + 4C_a & & S_i < \dfrac{S_{\mathrm{hom},i}}{2t} \end{pmatrix}$$

X_i : expansion rate of the i-th element

t : remodeling threshold

$S_{\mathrm{hom,i}}$: homeostatic stress of the i-th element (von Mises)

S_i : actual stress of the i-th element (von Mises)

C_a, C_b : remodeling constants

i : i-th element

then the sizes of the elements were expanded. However, the elements in which stresses were lower were reduced in sizes (Fig. 3). In Table 3 X_i was the expansion rate, $S_{hom,i}$ was the optimal von Mises equivalent stress for the normal element with number I. S_i was the actual von Mises equivalent stress of the abnormal element, t was the parameter related to the threshold and C_a and C_b were proportional constants. Between $S_{hom,i}$ / t and t * $S_{hom,i}$, as a tolerant state, the bone was assumed do not react to the stimulant stress.

No growth factor was taken into consideration for teeth, articular disk and cartilage, and changes were only made to bones.

In every remodeling the directions of the muscle forces were altered to the direction between the new positions of the insertion and the origin.

COSMOS/M (SRAC) was used for the basic analysis.

(3) Measurement of the mandibular morphology and bite force

12 patients (ages 13-28 years, 4 males and 8 females), who visited the Oral and Maxillofacial Surgery clinic, Shiga University of Medical Science from March 2000 to August 2001, had never undergone orthodontic treatment and did not have more than two large unrestored cavities, had their bite force and the area of occlusal contact area measured with Dental Prescale (Fuji Film co, Tokyo, Japan) by biting on the film for a maximum of three seconds.

Frontal and lateral cephalograms of these patients were photographed in order to examine the morphology of each mandibular bone, and the cephalograms used as follows.

The measuring points were selected as shown in Fig. 4.

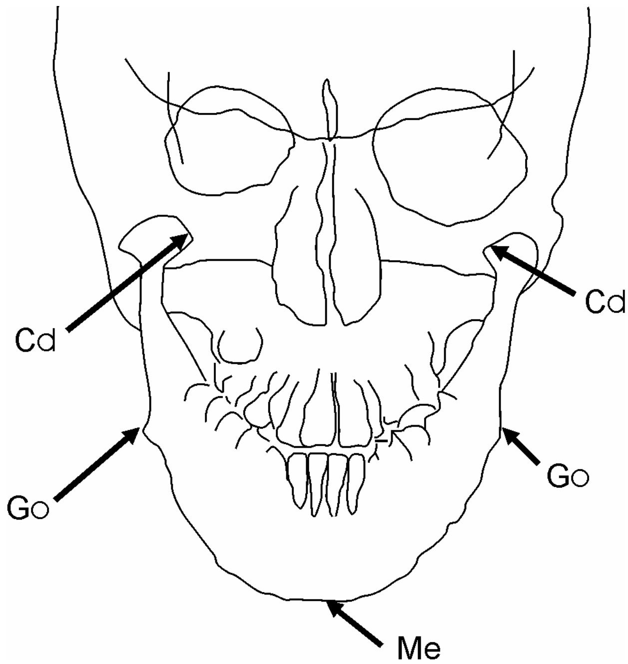

Cd	condylion	the most medial point of the condyle
Go	gonion	the most lateral point in the angle of the mandible
Me	menton	the lowest point of the mentalis

Fig. 4. Measuring points in mandible.

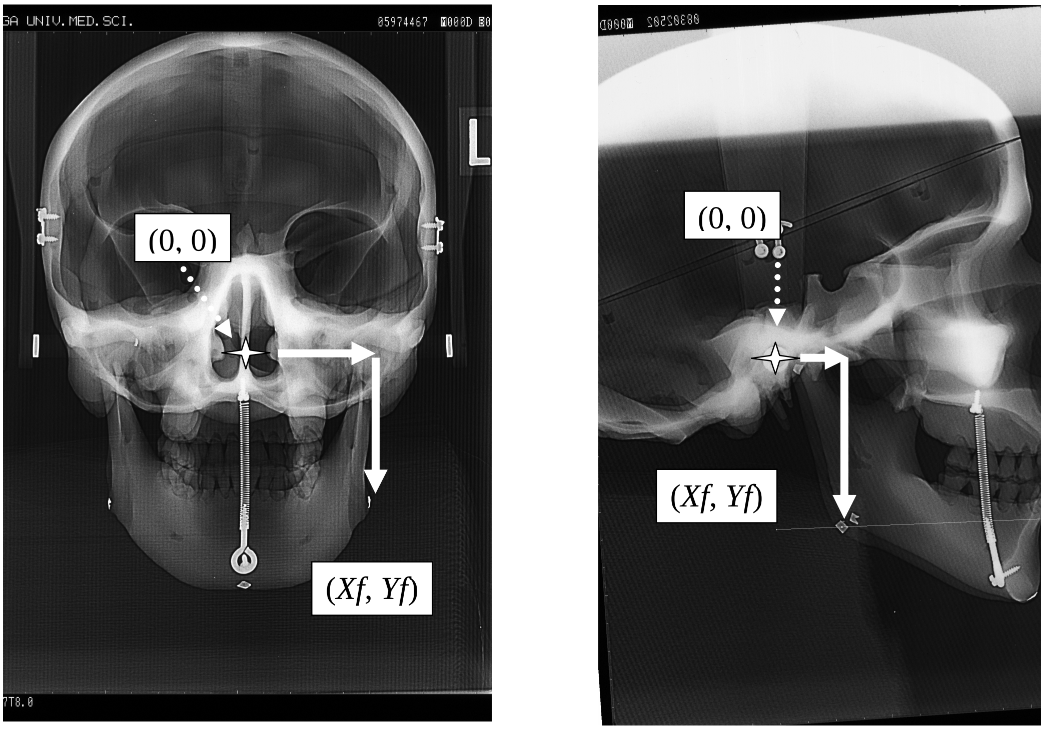

Fig. 5. Coordinates in cephalograms.

The three-dimensional coordinates of each measuring point were acquired. In the coordinate system the origin was the focus. The three-dimensional coordinate was constructed from two two-dimensional coordinates from frontal and lateral cephalograms. As frontal and lateral cephalograms of patients were not photographed at the same time, rotation of the head, centering on the ear rods might occur between the photographs. The angle of the rotation was obtained through measuring the positions of the upper incisor in these cephalograms. The lateral cephalograms were rotated by the angle centered on the ear rods to ensure placement at the same position as the frontal one, and so the coordinates of the measuring points were acquired (Fig. 5).

The X-ray device for the cephalograms was standardized as follows. The distance between the focus and the film was 1650 mm, the distance between the focus and the mid points of the left and right ear rods was 1500 mm, and when photographing the lateral cephalogram, the central axis of the X-ray passed through the center of the ear rods (Fig. 6).

Therefore, those coordinates in the ideal relationship are shown below:

$$Yl = \frac{1650y}{x},$$

$$Zl = \frac{1650z}{x},$$

$$Xf = \frac{1650}{1500 - y}(1500 - x),$$

$$Zf = \frac{1650}{1500 - y}z.$$

Yl and *Zl* – the coordinates in the rotated lateral cephalogram, where the origin is the center of the ear rod.

Xf and *Zf* – the coordinates in the frontal cephalogram, where the origin is the mid point of the left and right ear rods.

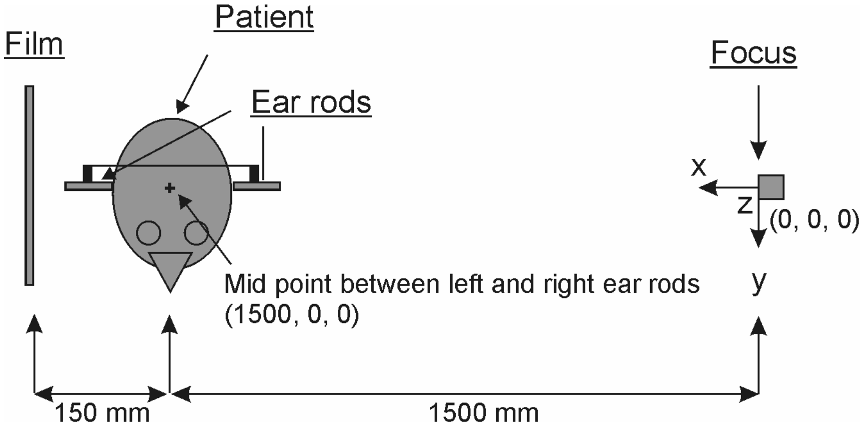

Fig. 6. 3-D coordinates in cephalometric X-ray device.

The values of x, y and z were computed as approximate values to the solution that fitted these equations. Here we have the coordinates of measuring points of which the origin was the focus when the lateral cephalogram was photographed.

A phantom experiment was carried out to examine these theoretical equations. In this experiment, a plastic model of a human head with small lead pieces stuck in the measuring points was used as a phantom. And also the values from cephalograms of a patient whose mandible was shifted to the left side; the menton was shifted 8 mm to the left in the frontal cephalogram were compared with the values which were derived from CT images (5 mm pitch helical CT, 1 mm re-sliced, SOMATOM PLUS4, Siemens).

(4) Asymmetry index

Asymmetry index (AI) was used to evaluate asymmetry of the bite force, the occlusal contact area and the morphology of the mandible.

Asymmetry Index(AI) =
= (left measurement – right measurement) / (left measurement + right measurement) ? 100 %

The results from the remodeling simulation were compared with patients with facial deformities to investigate the relationship between the morphology of the mandible and bite force. The form of the model’s mandible was evaluated using AI for differences between right and left in the distances between the condylion (Cd) and the menton (Me), and between the gonion (Go) and the menton (Me).

Von Mises equivalent stress was used as the models bite force per unit area occurring in the elements placed on the upper and lower teeth.

Results and discussion

Fig. 7 shows the stress distributions of the normal occlusion model and the malocclusion model (the ratio of occlusal contact area, right: left = 2.3:1, AI=-40; the ratio of muscle force, right: left = 1:1). In the normal model, the stress distribution was symmetric. In the malocclusion model, which had a difference of occlusal contact points, the stress on the right side increased more than on the left side in the maxilla. However, the stress on the left side increased more than on the right side in the mandible. The maxillofacial morphology as a result of the remodeling simulation of this malocclusion model is shown in Fig 8. The left half of the mandible was larger than the right side.

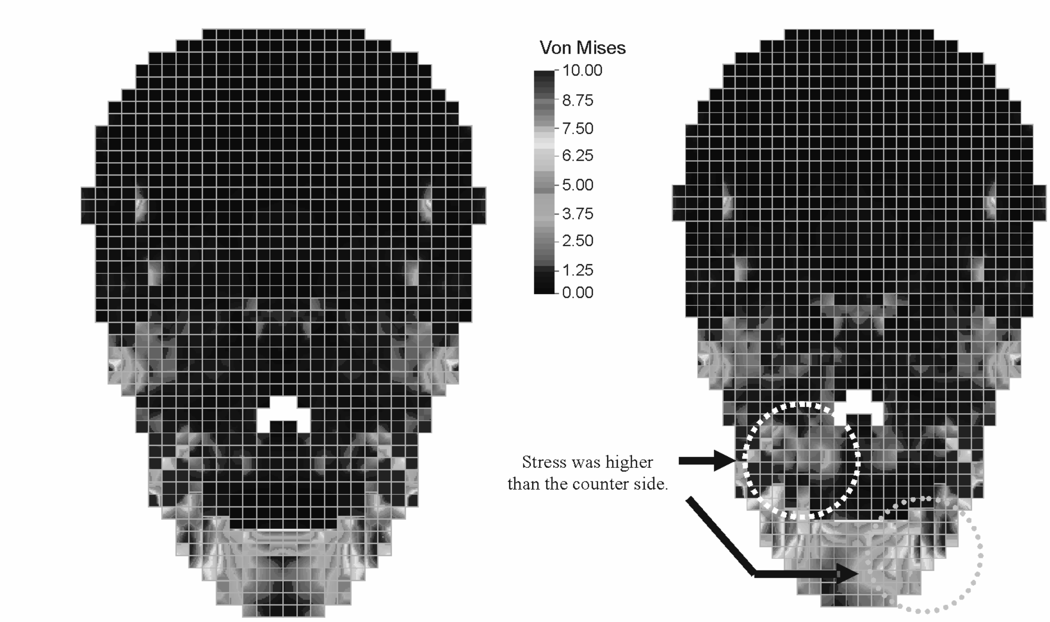

Normal occlusion model Malocclusion model

Fig. 7. Difference of stress distribution during clenching depends on occlusal condition.

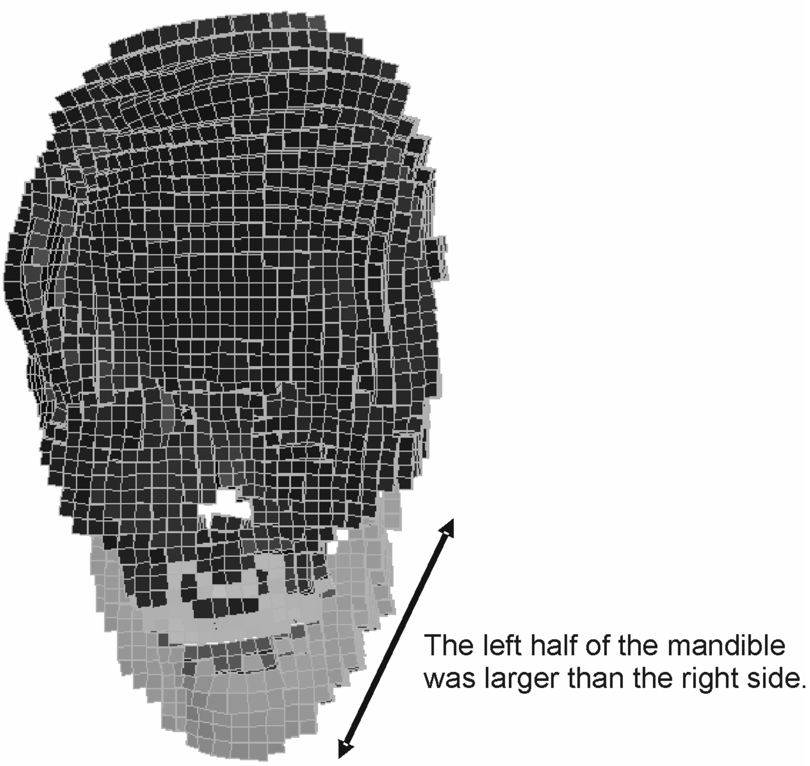

Fig. 8. A simulated facial deformity assumed by symmetric muscle forces and occlusal contact area 2.3 times larger on the right side than that on the left side.

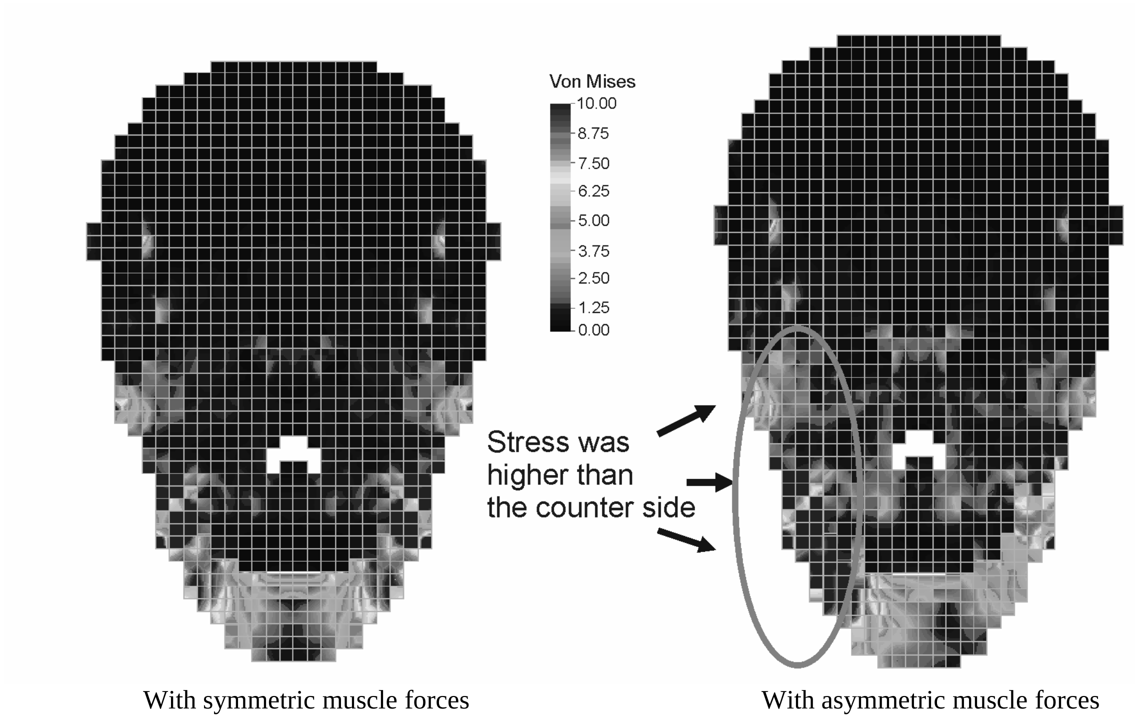

Fig. 9. Difference of stress distribution depends on asymmetric muscle forces.

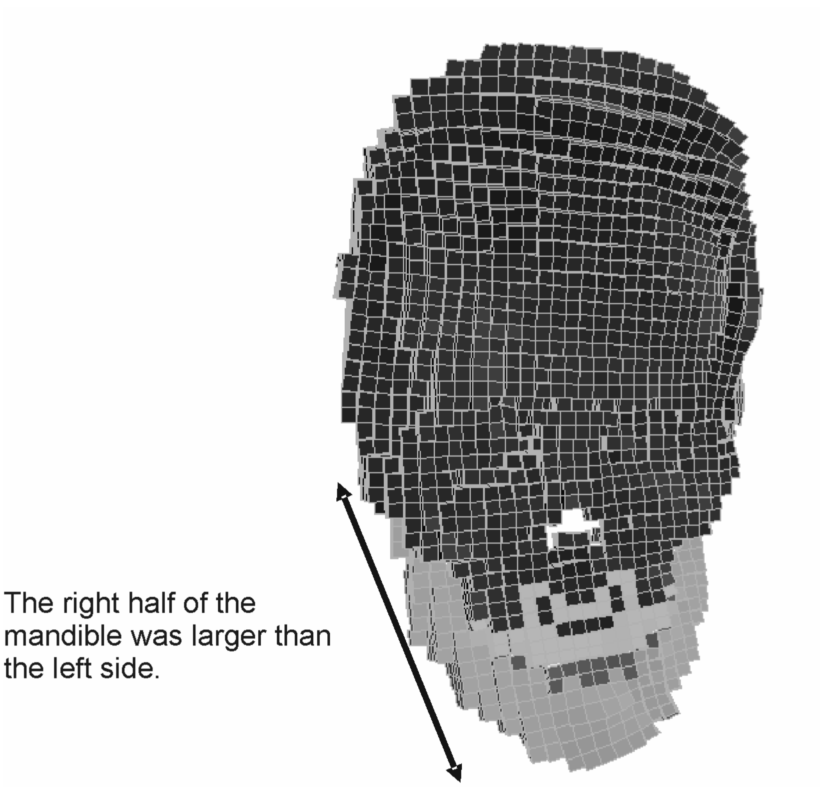

Fig. 10. A simulated facial deformity assumed by muscle forces 2 times larger on the right side than those on the left side and symmetric occlusal contact areas.

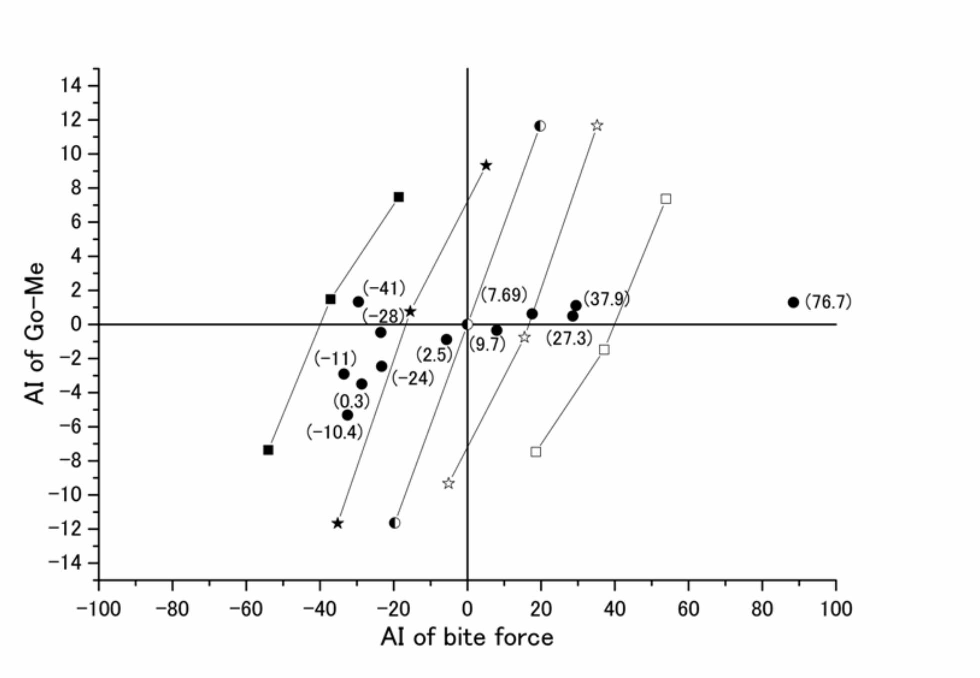

Fig. 11. Relationship between AI of bite force and AI of Go-Me in patient cases and simulated models.

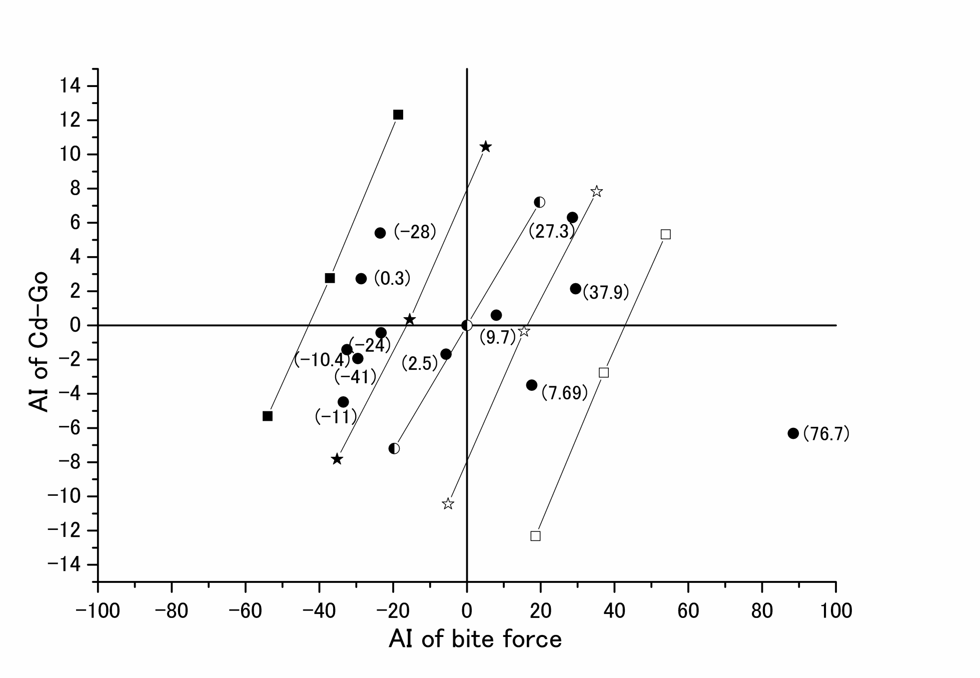

Fig. 12. Relationship between AI of bite force and AI of Cd-Go in patient cases and simulated models.

Symbols for Fig. 11 *and Fig.* 12*:* ★ *– simulated models whose AI of occlusal contact areas were –*16.7*;* ■ *– simulated models whose AI of occlusal contact areas were –*40*;* ◐ *– simulated models whose AI of occlusal contact areas were* 0*;* □ *– simulated models whose AI of occlusal contact areas were* 40*;* ☆ *– simulated models whose AI of occlusal contact areas were* 16.7*;* ● *– patients.*
AI of occlusal contact areas were individually shown in parentheses .

Fig. 9 shows the stress distribution of the normal occlusion model with symmetric and with asymmetric muscle forces (the ratio of occlusal contact area, right: left = 1 : 1, AI=0; the ratio of muscle force, right: left = 2: 1). In the model with muscle forces 2 times larger on the right side than on the left side, the stress in the right side increased more than in the left side in the maxilla and mandible. The result of the remodeling simulation of this model is shown in Fig 10. The right half of the mandible was larger than the left side.

The result of the phantom experiment is shown in the Table 4. The relative errors of the measured values of the phantom from the frontal and lateral cephalograms to those measured with a vernier caliper were -1.79% minimum, 0.67% maximum. The relative errors to the values measured with CT images were –0.62% minimum, 0.06% maximum (Table 5).

Table 4. Relative error of values from X-ray cephalograms to measurement values of the phantom.

	Phantom(mm)	Cephalograms	Error(%)
Right Cd-Go	57.81	58.20	0.67%
Right Go-Me	78.10	77.20	-1.15%
Left Cd-Go	52.79	51.85	-1.79%
Left Go-Me	80.68	79.90	-0.96%

Table 5. Comparison between values from CT and from cephalograms.

	CT (mm)	Cephalograms	Error(%)
Right Cd-Go	52.20	51.87	-0.62%
Right Go-Me	86.39	86.13	-0.29%
Left Cd-Go	51.74	51.78	0.06%
Left Go-Me	82.24	81.75	-0.59%

The mandible morphology, the occlusal contact area, and the bite forces of the results of the remodeling simulation and of the patients are shown in Fig. 11, 12.

As the result of the remodeling simulation, the distance between the nodes at Cd and Go and the distance between the nodes at Go and Me on one side increased as the bite force on the same side increased more than on the other side. In the graph the symbols of models whose left side occlusal contact area were larger than of the right side tended to be more located in the right area than the symbols of models whose right side occlusal contact area were larger than of the left side. The lines of malocclusion models tended to go away from the lines of normal occlusion models as increasing the imbalance of the occlusal contact areas. The result of the remodeling simulation was similar to the relationship between condylion-gonion(Cd-Go) and gonion-menton (Go-Me) of the patients and of the bite force.

Nakamura [12] reported deformation of condyles in the growing process caused by extracting the upper and lower molars of young Wister rats, and considered that it was the result of the changing the direction and magnitude of the loads to the condyles. Nakamura [13] showed that the craniomaxillofacial asymmetry was made by continuous oppression exerted by external forces in the period of growth to the unilateral maxilla and occipital bones of rats. Morikawa [10] showed that malocclusion and deformity of condyles were produced as a result of growth suppression of the unilateral skull and maxilla of young rats, and considered that it was the result of the changes of loads on condyles. These results indicate that the abnormal stresses in the maxillofacial complex cause abnormal growth. In humans, there exist some case reports [2, 7] in which maxillofacial asymmetry was exacerbated in periods of puberty growth, but the detailed mechanism was not made clear. We could not find any reports of the relationship between stress distribution and deformity using a three-dimensional finite element method of a human maxillofacial model that included the skull. Therefore, examination on the relation between stress and deformation using human models is necessary.

Observations of the stress distribution of the maxillofacial region under clenching loads have been done using strain gauge methods, a photoelastic approach, etc [24]. But by these methods, it is hard to obtain a form that adapts to the load. The finite element method is a numerical calculation method for detailed stress distribution, and is also suitable for obtaining forms those adapted to the load [20, 22, 23].

Our remodeling simulation using the three-dimensional finite element method was carried out according to Wolff's law [1, 21], in which bones receiving higher stress grow more and those receiving lower stress were reduced in sizes. These remodeling expressions consisted of smooth continuous functions to express the property of the organism.

Using this hypothetic theoretical equation of bone remodeling, we obtained a form that was very similar to the theoretical solution of the cantilever beam with an equal intensity [11,22]. This indicated that equation was appropriate to obtain the optimal form for the stress. When a stronger muscle force was set, the form of model showed features of prehistoric humans who masticated harder food than modern humans, a large mandible, an overhang of the zygomatic region, a leveling of the upper margin of the orbit, a projection of the mental region and a projection of the glabella and the nasal bones [3,4,11]. This fact suggests that this equation is applicable to bone remodeling of the maxillofacial region.

As a result of this simulation, Cd-Go and Go-Me increased as the bite force increased. This was similar to the relationship between bite force and the distance between Cd-Go and Go-Me of the patients. This suggests that an asymmetry of mandible might occur from an imbalance of the stress distribution with a dysfunction of occlusion through the remodeling according to our hypothesis in which the portion of the bone of which stress increased should be expanded, that the portion of the bone of which stress decreased should be reduced. Haraguchi et al [2] and Kobayashi et al [7] reported cases in which the mandible shift was exacerbated through puberty growth. Satoh [16] considered that it was necessary to recover rapidly the harmony of muscle function of right and left when it is suspected that there was such a difference of masseter function between right and left during a period of growth, because of the difference in the shapes of the condyles between right and left caused by giving a difference to the masseter function of rats. However, in order to prevent maxillofacial asymmetry, just keeping the symmetry of the masseter force is not sufficient, it seems necessary to also pay attention to occlusal condition. As shown in Fig. 7, even if masticatory muscle forces are symmetric, an asymmetric stress has been generated in the maxillofacial complex if the occlusal condition is asymmetric. It is considered that this simulates the case of a crossbite. There are some case reports of patients who presented with malocclusion and crossbites [7, 15], and that the mandible shift was exacerbated through puberty growth. The simulation results indicate that the lack of occlusal contacts according to crossbites might be a factor that constructs dynamic conditions those cause asymmetrical mandibular growth.

Clenching while asleep generates much larger bite forces than those usual masticatory ones [6]. When clenching occurs under conditions of an imbalanced occlusion and/ or imbalanced muscle force, the stress distribution in the maxillofacial bone is asymmetrical. This asymmetrical stress distribution is suspected to induce maxillofacial bone asymmetrical growth.

Conclusions

1. A remodeling simulation was carried out to examine the possibility that a dysfunction of a mandible with malocclusion and/ or asymmetrical muscle forces might cause maxillofacial asymmetry. The results of this simulation were compared with patients having maxillofacial deformity.
2. As a result the distances Cd-Go and Go-Me increased with increasing bite force, which was almost equal to the relationship between the bite force and the mandible morphology of the patients.
3. From the remodeling according to Wolff's law, we suggest that the asymmetry of the distances Cd-Go and Go-Me might occur from an imbalance of the stress distribution with occlusal dysfunction. In order to prevent maxillofacial asymmetry, just keeping the symmetry of the masseter force is insufficient, it seems necessary to also pay attention to the occlusal condition.

Acknowledgement

We thank Ryusuke Nakai and Dr. Hiroaki Yoshida of Department of Medical Simulation Engineering, Institute for Frontier Medical Sciences and Rikiya Kikumoto, Jin Itoh and Hiroshi Inoue of Department of Radiology, Otowa Hospital, and Mitsuru Komizu of Department of Radiology, Shiga University of Medical Science Hospital for their support.

References

1. Asada K. The glossary of biomechanics. In: Shimazu A., Asada K. (Editor), **Biomechanical Orthopaedics**, 2nd Edition. Tokyo, Kanehara CO, 493, 1994 (in Japanese).
2. Haraguchi Y. Nakata S. et al. Functional analysis of masticatory muscle in a patient with progressing facial asymmetry. **J Jpn Ortho Soc**, 53(2): 183-191, 1994 (in Japanese).
3. Ikeda J. The origin of Japanese people. In: **The root by which the Japanese came.** Tokyo, Asahi Shinbun CO, 104-114, 1998 (in Japanese).
4. Itoh G. Adaptation of the hard tissue of the masticatory system to soft foods. In: Kubota K. (Editor). **Formation and adaptation of the masticatory system**. Tokyo, Huujinsya CO, 231-239, 1988 (in Japanese).
5. Kamijoh Y. 3 Mm.masticatorii. In: 2 Myologia. **Oral anatomy**, 13th Ed. Tokyo, Anatome CO, 252-262. 1970 (in Japanese).
6. Kobayashi Y. Bruxism. 8 The physiology of the temporomandibular joint. In: Uemura S., Sugisaki M. et al. (Editor). **The small dictionary of Temporomandibular joint**. Tokyo, Nippon dental review CO, 166, 1990 (in Japanese).
7. Kobayashi M., Saitoh I. et al. Long–term observation of mandibular protrusion cases worsen in pubertal growth spurt. **J Jpn Ortho Soc,** 55(3): 234-245, 1996 (in Japanese).
8. Korioth,T. W. P. Hannam A. G. Effect of bilateral asymmetric tooth clenching on load distribution at the mandibular condyles. **J Prosthet Dent**, 64: 62-73, 1990.
9. Korioth Tom W.P., Hannam Alan G. Mandibular forces during simulated tooth clenching. **J Orofacial Pain,** 8(2): 178-189, 1994.
10. Morikawa M. Effect of Experimental inhibition of craniomaxillofacial growth on the rat condyle. **J Osaka Odontol Soc,** 58(1): 57-67, 1995 (in Japanese).
11. Nakai R., Tsutsumi S. et al. The simulation of adaptive bone remodeling on maxillofacial bone caused by occlusal force. **Journal of Japanese society for clinical biomechanics,** 22: 369-373, 2001 (in Japanese).
12. Nakamura T. Influence of molar extraction on the development of mandibular condyles of rats. **Hokkaido J Dent Sci,** 13: 123-142, 1992 (in Japanese).
13. Nakamura Y. Effect of Unilateral Craniomaxillofacial Deformity on Rat Mandibular Growth and Development. **J Osaka Odontol Soc,** 56(6): 509-523, 1993 (in Japanese).
14. Huiskes R., Weinans H., et al. Adaptive bone-remodeling theory applied to prosthetic-design analysis. **J Biomechanics,** 20(11/12): 1135-1150, 1987.
15. Sakuda M., Nakago T. et al. A case of posterior cross-bite: changes in form and function following orthodontic treatment. **J Jpn Ortho Soc,** 28(2): 329-343, 1969 (in Japanese).

16. Satoh Y. Influence of asymmetry in the function of masseter muscle on the growing mandibular condyles. **J Osaka Univ Dent Soc**, 31: 137-164, 1986 (in Japanese).
17. Takakuda K. Experimental study on adaptive remodeling of bone. **Clinical Orthopaedic Surgery**, 33(8): 963-969, 1998 (in Japanese).
18. Tanaka E. Stress distribution in the TMJ during clenching. **J Osaka Univ Dent Soc,** 38(1): 131-160, 1993 (in Japanese).
19. Tsuruki T. Orthognathic surgery. In: Sasaki M (Editor). **Maxillofacial and Oral surgery.** Tokyo, Oral health association of Japan, 612, 1995 (in Japanese).
20. Tsutsumi S. Biomechanical Simulation of Bone Remodeling in Dentistry, ASME **Tissue Engineering**, 14: 59-62, 1989.
21. Tsutsumi S. Wolff's law. **The bone,** 8(3): 101-108, 1994 (in Japanese).
22. Tsutsumi S. and Doi K. Pseudo-3D Computer Simulation for Pathogenesis and Rehabilitation Cervical Spine Deformity by Malocclusion. **International Journal of Industrial Ergonomics**, 9(2): 137-144, 1992.
23. Tsutsumi S., Inoue Y. and Yamamuro T. Computer Simulation of Bone Remodeling in Dentistry and Orthopaedics. **Wolff's Law and Connective Tissue Regulation.** Regling, G. (ed.), de Gruyter (Berlin), 103-112, 1992.
24. Yoshida K. The strain gauge method. In: Shimazu A., Asada K., (Editor). **Biomechanical Orthopaedics**, 2nd Edition. The explanation of the biomechanics technique. Tokyo, Kanehara CO, 455, 1994 (in Japanese).

ПАТОМЕХАНИКА ЧЕЛЮСТНО-ЛИЦЕВОЙ АСИММЕТРИИ: КОМПЬЮТЕРНОЕ МОДЕЛИРОВАНИЕ АДАПТИВНОЙ ПЕРЕСТРОЙКИ КОСТНОЙ ТКАНИ

М. Кутсуки, Я. Ямагучи, К. Иошитаке, Т. Азума, С. Цуцуми
(Киото, Япония)

Исследуется связь между челюстно-лицевой асимметрией, условиями смыкания зубов и силой кусания. Моделирование производится методом конечных элементов с помощью закона Вольфа. Проводится сравнение результатов по вычислению асимметрии нижней челюсти, силы кусания и окклюзионных поверхностей для четырех типов анормальной окклюзии и нормальной окклюзии. Сравнение с клиническими наблюдениями показывает хорошее соответствие. Высказывается предположение, что асимметрия челюстно-лицевой области является следствием несимметричного распределения напряжений и усилий в жевательных мышцах.

Ключевые слова: биомеханика зубо-челюстной системы, асимметрия челюстно-лицевой системы, патологический прикус, закон Вольфа, метод конечных элементов

Received 01 December 2001